

# Efficient passively Q-switched Nd:YLF TEM<sub>00</sub>-mode laser at 1053 nm: selection of polarization with birefringence

Y.J. Huang · C.Y. Tang · W.L. Lee · Y.P. Huang ·  
S.C. Huang · Y.F. Chen

Received: 11 November 2011 / Revised version: 19 December 2011 / Published online: 21 March 2012  
© Springer-Verlag 2012

**Abstract** The natural birefringence of the Nd:YLF crystal is utilized to achieve a reliable TEM<sub>00</sub>-mode linearly polarized laser at 1053 nm in a compact concave-plano resonator. The efficient selection of the polarization relies on the combined effect of the difference in diffraction angle for  $\sigma$ - and  $\pi$ -polarization of a wedged laser crystal and the alignment sensitivity of an optical resonator. We further employ a Cr<sup>4+</sup>:YAG saturable absorber to perform the passively Q-switched operation. At an incident pump power of 12 W, the maximum average output power is up to 2.3 W with a pulse repetition rate of 8 kHz and a pulse width of 9 ns. The pulse energy and peak power are found to be 288  $\mu$ J and 32 kW, respectively.

## 1 Introduction

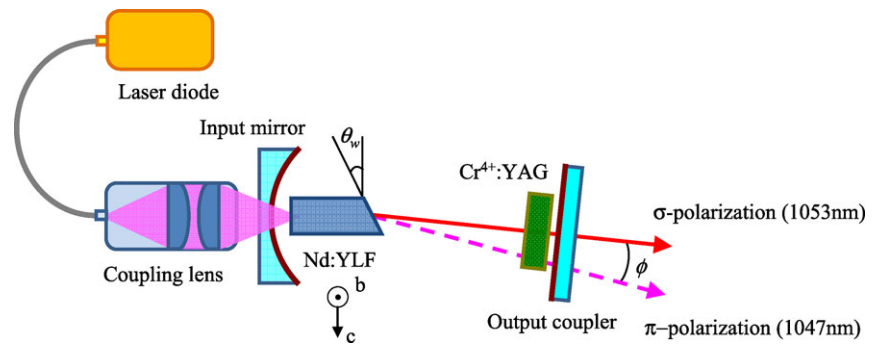
Passive Q-switching has been widely exploited to accomplish compact diode-pumped all solid-state pulsed lasers [1–9]. A long upper-state lifetime of the gain medium is highly desirable for continuously pumped passively Q-switched (PQS) lasers to generate large amounts of pulse energies. As a consequence, the Nd:YLF crystal with a relatively long upper-state lifetime is usually expected to be appropriate for the construction of a high-pulse-energy laser with the Cr<sup>4+</sup>:YAG crystal as a saturable absorber [10–12]. Another attractive feature of the Nd:YLF crystal is the emission line at 1053 nm, which makes it useful in developing the master oscillator for a Nd:glass power amplifier [13].

Although it is generally convenient to employ the c-cut Nd:YLF crystal as a gain medium for generating a 1053-nm laser [14–16], the isotropic property in the transverse plane typically leads the polarization state not to be linearly polarized. The a-cut Nd:YLF crystal can alternatively be employed to obtain a linearly polarized output. However, the stimulated emission cross section at 1047 nm is higher than that at 1053 nm by a factor of 1.5 for the a-cut Nd:YLF crystal [17–22]. As a result, suppressing the  $\pi$ -polarized emission at 1047 nm turns into an important issue in designing a linearly-polarized 1053-nm laser with the a-cut Nd:YLF crystal. It has been shown that the effects of extra losses may be enhanced by the energy transfer upconversion (ETU) which causes a reduction in the effective upper laser level lifetime and an increase in fractional thermal loading [23, 24]. Therefore, it is practically important to develop an approach without introducing considerable extra losses for achieving an efficient linearly polarized Nd:YLF 1053-nm pulsed laser.

In a previous study [25], it was demonstrated that the selection of the polarization in an a-cut Nd:YVO<sub>4</sub> laser could be attained by combining the birefringence of the laser crystal with the alignment sensitivity of the plano-plano resonator. In this work, we exploit the birefringence of the a-cut Nd:YLF crystal to realize the selection of the polarization in a compact concave-plano resonator. Note that the plano-plano cavity is generally not appropriate for the Nd:YLF laser because the gain medium has a negative temperature coefficient for the refractive index, leading to a defocussing lens. We experimentally find that a reliable linearly polarized TEM<sub>00</sub>-mode laser at 1053 nm can be achieved in a cavity as short as 5 cm by using an a-cut Nd:YLF crystal with a wedged angle of 3°. We further use a Cr<sup>4+</sup>:YAG saturable absorber with an initial transmission of 80 % to investigate the performance of the PQS operation for vari-

Y.J. Huang · C.Y. Tang · W.L. Lee · Y.P. Huang · S.C. Huang ·  
Y.F. Chen (✉)  
Department of Electrophysics, National Chiao Tung University,  
1001 TA Hsueh Road, Hsinchu 30050, Taiwan  
e-mail: yfchen@cc.nctu.edu.tw  
Fax: +886-35-725230

**Fig. 1** Schematic of the cavity setup for a diode-pumped PQS Nd:YLF/Cr<sup>4+</sup>:YAG laser



ous output couplings. With an output coupling of 30 %, the maximum output power of 2.3 W is generated at an incident pump power of 12 W, where the pulse repetition rate and pulse width are 8 kHz and 9 ns, respectively. The corresponding pulse energy and peak power are calculated to be up to 288  $\mu\text{J}$  and 32 kW, respectively. To the best of our knowledge, the pulse energy and peak power are the highest ever reported among the continuously diode-end-pumped PQS Nd-doped crystal lasers with the Cr<sup>4+</sup>:YAG crystal of the same initial transmission.

## 2 Experimental setup

The experimental setup is schematically shown in Fig. 1. The input mirror was a concave mirror with the radius-of-curvature of 500 mm. It was antireflection (AR) coated at 806 nm on the entrance face, and was coated for high transmission at 806 nm as well as for high reflection at 1053 nm on the second surface. The gain medium was a 0.8 at% a-cut Nd:YLF crystal with dimensions of  $3 \times 3 \times 20 \text{ mm}^3$ , and it was placed to be adjacent to the input mirror. Both facets of the laser crystal were AR coated at 806 nm and 1053 nm. The second surface of the laser crystal was wedged at an angle  $\theta_w = 3^\circ$  with respect to the first surface, as indicated in Fig. 1. The Cr<sup>4+</sup>:YAG saturable absorber with the initial transmission of 80 % was AR coated at 1053 nm on both surfaces, and it was placed near to the output coupler. The laser crystal and the saturable absorber were wrapped with the indium foil and mounted in water-cooled copper heat sinks at 20 °C. The pump source was a 15-W fiber-coupled laser diode at 806 nm with a core diameter of 400  $\mu\text{m}$  and a numerical aperture of 0.2. The pump beam was reimaged into the laser crystal with a lens set that has the focal length of 25 mm and the coupling efficiency of 90 %. The flat output couplers with the transmission of 10 %, 20 %, 30 %, 36 %, and 50 % were utilized for systematic investigations on the laser characteristics during the experiment. The cavity length was set to be 50 mm for the construction of a compact laser. With the ABCD-matrix theory, the cavity mode radii inside the laser crystal and the saturable absorber were estimated to be approximately 236  $\mu\text{m}$  and 224  $\mu\text{m}$ , respectively.

The pulse temporal behaviors were recorded by a LeCroy digital oscilloscope (Wavepro 7100, 10 G samples/s, 1 GHz bandwidth) with a fast Si photodiode.

## 3 Performance of CW and PQS operations

First of all, we explore the angle tuning characteristics of the Nd:YLF laser for the  $\sigma$ - and  $\pi$ -polarization in the CW operation, where the Cr<sup>4+</sup>:YAG saturable absorber was removed, the transmission of the output coupler was chosen to be 30 %, and the incident pump power was fixed to be 12 W to avoid the possibility of the thermal fracture in the laser crystal. As shown in Fig. 2(a), the output polarization state can be easily switched by simply tilting the orientation of the output coupler. Note that the tilting angle  $\phi$  is defined as the included angle with respect to the orientation of the output coupler corresponding to the maximum output power at 1053 nm, as depicted in Fig. 1. The angular separation between the  $\sigma$ - and  $\pi$ -polarization under the individual maximum output power is experimentally found to be around 1.153 mrad; that is, the angular separation between the point b and c indicated in Fig. 2(a) is approximately 1.153 mrad. On the other hand, the refractive indices for the  $\sigma$ - and  $\pi$ -polarization in the a-cut Nd:YLF crystal are  $n_\sigma = 1.448$  and  $n_\pi = 1.47$ , respectively. With the Snell's law under the small-angle approximation, we can theoretically derive an angular separation to be  $(n_\pi - n_\sigma)\theta_w \sim 1.152 \text{ mrad}$  between the two polarizations external to the wedged crystal, which is in a good agreement with the experimental observations. The two-dimensional spatial distributions for the  $\sigma$ - and  $\pi$ -polarization under the individual maximum output power are recorded with a digital camera, and both are found to display a near-diffraction-limited TEM<sub>00</sub> transverse mode, as shown in Fig. 2(b) for the case of  $\sigma$ -polarization.

With the optimal alignment for 1053-nm emission, we made a thorough study on the output power with respect to the output coupling at an incident pump power of 12 W. Note that the polarization extinction ratio at 1053 nm is considerably larger than 100:1 once the cavity was aligned for the

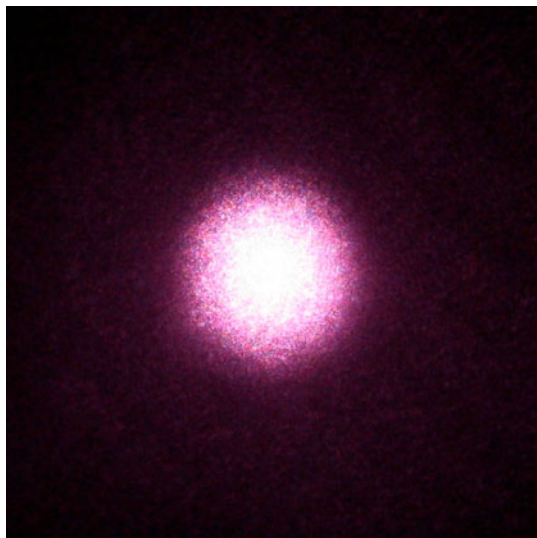
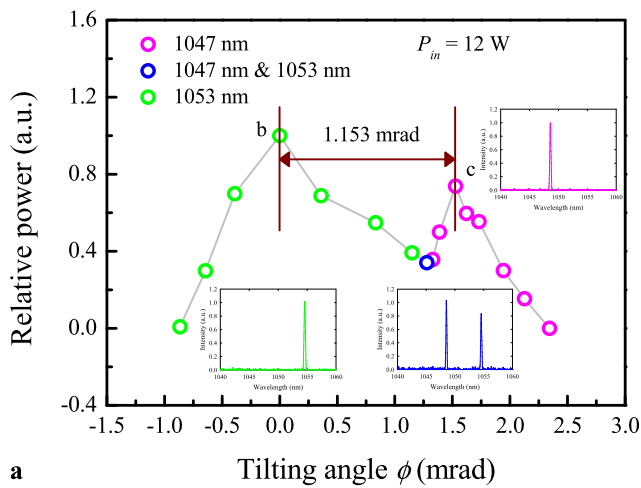


**Fig. 2** (a) The angle tuning characteristics of the 3°-wedged a-cut Nd:YLF laser for the  $\sigma$ - and  $\pi$ -polarization in the CW operation; (b) The two-dimensional spatial distributions for the  $\sigma$ -polarization under the maximum output power, indicating a near-diffraction-limited TEM<sub>00</sub> transverse mode

optimization at 1053 nm. The output power in the CW operation is experimentally found to decrease from 4.88 W to 2.45 W with increasing the output coupling from 10 % to 50 %, as revealed by the red curve in Fig. 3.

When the Cr<sup>4+</sup>:YAG saturable absorber was inserted into the laser cavity, the dependence of the output power in the PQS operation on the output coupling is demonstrated by the green curve in Fig. 3. Experimental results reveal that at an incident pump power of 12 W, the maximum output power of 2.3 W is achieved with the output coupling of 30 % in the PQS operation. The optical-to-optical conversion efficiency from 806 nm to 1053 nm is thus evaluated to be 18.3 %. Figure 4 illustrates the pulse repetition rate and the pulse width versus the output coupling in the PQS operation. It is

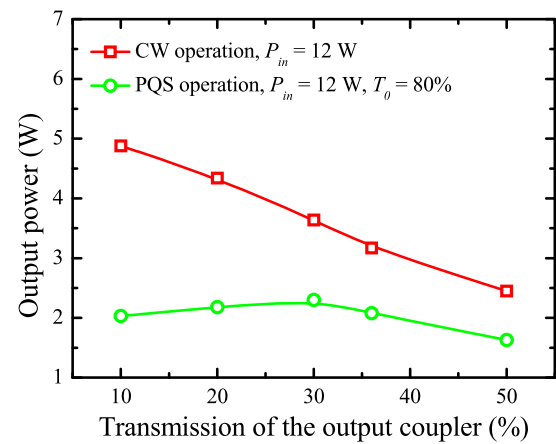


**Fig. 3** The maximum output powers at 1053 nm in the CW and PQS operations as a function of the output coupling

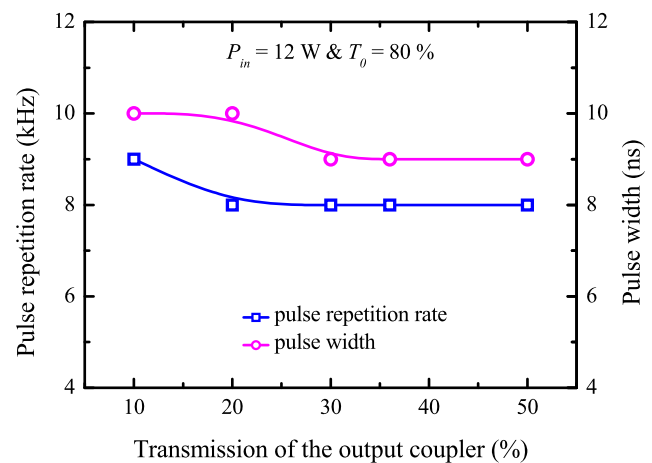


**Fig. 4** Dependences of the pulse repetition rate and pulse width on the output coupling

experimentally found that both the pulse repetition rate and the pulse width are insensitive to the change of the output coupling; namely, when the transmission of the output coupler is varied between 10–50 %, the pulse repetition rate and the pulse width are in the ranges 8–9 kHz and 9–10 ns, respectively. According to the experimental results illustrated in Figs. 3 and 4, the pulse energy and peak power are calculated as a function of the transmission of the output coupler, as depicted in Fig. 5. For the output coupler with the transmission of 30 %, the pulse energy and the peak power as high as 288  $\mu$ J and 32 kW are achieved at an incident pump power of 12 W. It is worthwhile to mention that so far the pulse energies obtained with the continuously diode-end-pumped PQS Nd-doped crystal/Cr<sup>4+</sup>:YAG lasers, such as the Nd:YAG [1, 3], c-cut Nd:YLF [7], Nd-doped vanadate crystals [1–6, 8, 9], are not more than  $\sim$ 210  $\mu$ J. That is to say, the pulse energy based on the  ${}^4F_{3/2} \rightarrow {}^4I_{11/2}$  transition is greatly enhanced in our cavity design. Figures 6(a)–6(b) show the typical oscilloscope traces of the

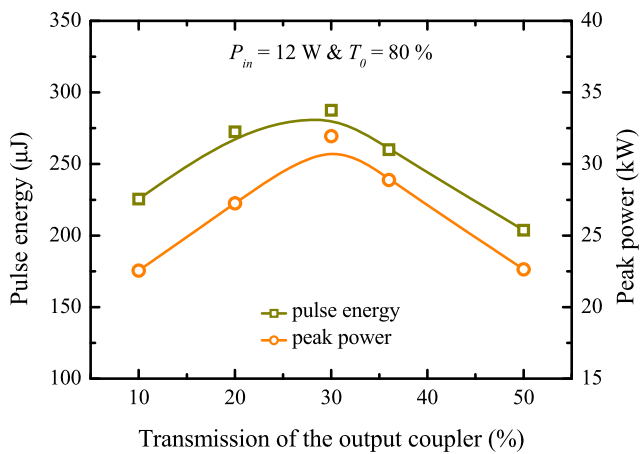


**Fig. 5** Dependences of the pulse energy and peak power on the output coupling

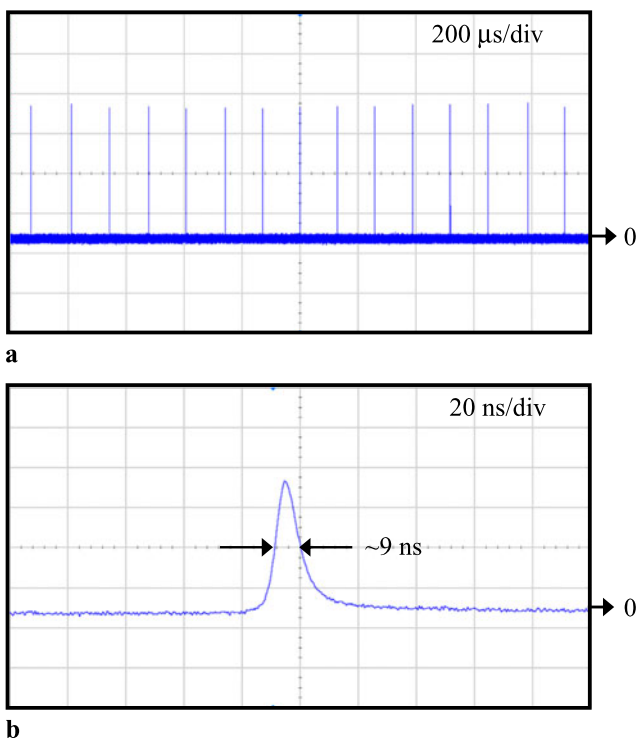


**Fig. 6** Typical temporal behaviors at 1053 nm with: (a) time span of 2 ms, and (b) time span of 200 ns, which were recorded with the output coupling of 30 % under an incident pump power of 12 W

output pulses at 1053 nm with the time span of 2 ms and 200 ns, respectively. The temporal behaviors were recorded with the output coupling of 30 % under an incident pump power of 12 W. The pulse-to-pulse amplitude fluctuation is found to be better than  $\pm 2\%$ . With a knife-edge method, the beam quality factors at 1053 nm for the orthogonal directions were measured to be  $M_x^2 < 1.1$  and  $M_y^2 < 1.15$ , respectively.

## 4 Conclusion

In summary, we have successfully demonstrated a reliable TEM<sub>00</sub>-mode linearly polarized laser at 1053 nm with the natural birefringence of a wedged Nd:YLF crystal in a compact concave-plano cavity. Using the Cr<sup>4+</sup>:YAG saturable absorber to perform PQS operation, the maximum output power can be up to 2.3 W under an incident pump power of 12 W. Under this output condition, the pulse repetition rate and the pulse width are found to be 8 kHz and 9 ns, respectively. The corresponding pulse energy and the peak power are up to 288 μJ and 32 kW, respectively. We believe that the relatively compact configuration presented here is potentially useful for the generation of high-peak-power pulses in Q-switched Nd:YLF lasers at 1053 nm.

**Acknowledgements** The authors thank the National Science Council for their financial support of this research under Contract No. NSC-100-2628-M-009-001-MY3.

## References

1. A. Agnesi, S. Dell'Acqua, C. Morello, G. Piccinno, G.C. Reali, Z. Sun, *IEEE J. Sel. Top. Quantum Electron.* **3**, 45 (1997)
2. Y. Bai, N. Wu, J. Zhang, J. Li, S. Li, J. Xu, P. Deng, *Appl. Opt.* **36**, 2468 (1997)
3. A. Agnesi, S. Dell'Acqua, E. Piccinini, G. Reali, G. Piccinno, *IEEE J. Quantum Electron.* **34**, 1480 (1998)
4. C. Li, J. Song, D. Shen, N.S. Kim, J. Lu, K. Ueda, *Appl. Phys. B* **70**, 471 (2000)
5. J. Liu, Z. Wang, X. Meng, Z. Shao, B. Ozygus, A. Ding, H. Weber, *Opt. Lett.* **28**, 2330 (2003)
6. J. Liu, B. Ozygus, S. Yang, J. Erhard, U. Seelig, A. Ding, H. Weber, X. Meng, L. Zhu, L. Qin, C. Du, X. Xu, Z. Shao, *J. Opt. Soc. Am. B* **20**, 652 (2003)
7. S. Pan, K. Han, H. Wang, X. Fan, J. He, *Chin. Opt. Lett.* **4**, 407 (2006)
8. H. Yu, H. Zhang, Z. Wang, J. Wang, Y. Yu, Z. Shao, M. Jiang, *Opt. Lett.* **32**, 2152 (2007)
9. F.Q. Liu, H.R. Xia, S.D. Pan, W.L. Gao, D.G. Ran, S.Q. Sun, Z.C. Ling, H.J. Zhang, S.R. Zhao, J.Y. Wang, *Opt. Laser Technol.* **39**, 1449 (2007)
10. X. Peng, L. Xu, A. Asundi, *IEEE J. Quantum Electron.* **41**, 53 (2005)
11. D. Li, Z. Ma, R. Haas, A. Schell, P. Zhu, P. Shi, K. Du, *Opt. Lett.* **33**, 1708 (2008)
12. N.U. Wetter, E.C. Sousa, F.D.A. Camargo, I.M. Ranieri, S.L. Baldochi, *J. Opt. A* **10**, 104013 (2008)
13. A.V. Okishev, W. Seka, *IEEE J. Sel. Top. Quantum Electron.* **3**, 59 (1997)
14. J.M. Auerbach, R.L. Schmitt, *Opt. Lett.* **16**, 1171 (1991)
15. S.D. Pan, J.L. He, Y.E. Hou, Y.X. Fan, H.T. Wang, Y.G. Wang, X.Y. Ma, *IEEE J. Quantum Electron.* **42**, 1097 (2006)
16. Y. Sun, H. Zhang, Q. Liu, L. Huang, Y. Wang, M. Gong, *Laser Phys. Lett.* **7**, 722 (2010)
17. T.M. Pollak, W.F. Wing, R.J. Grasso, E.P. Chicklis, H.P. Jenssen, *IEEE J. Quantum Electron.* **18**, 159 (1982)
18. J.E. Murray, *IEEE J. Quantum Electron.* **19**, 488 (1983)
19. G. Cerullo, S.D. Silvestri, V. Magni, *Opt. Commun.* **93**, 77 (1992)

20. B. Frei, J.E. Balmer, *Appl. Opt.* **33**, 6942 (1994)
21. W.A. Clarkson, P.J. Hardman, D.C. Hanna, *Opt. Lett.* **23**, 1363 (1998)
22. C. Bollig, C. Jacobs, M.J.D. Esser, E.H. Bernhardt, H.M.V. Bergmann, *Opt. Express* **18**, 13993 (2010)
23. P.J. Hardman, W.A. Clarkson, G.J. Friel, M. Pollnau, D.C. Hanna, *IEEE J. Quantum Electron.* **35**, 647 (1999)
24. L.C. Courrol, E.P. Maldonado, L. Gomes, N.D. Vieira Jr, I.M. Ranieri, S.P. Morato, *Opt. Mater.* **14**, 81 (2000)
25. A. Agnesi, S. Dell'Acqua, *Appl. Phys. B* **76**, 351 (2003)